

# Polarized Hyphal Growth in *Candida albicans* Requires the Wiskott-Aldrich Syndrome Protein Homolog Wal1p<sup>†</sup>

A. Walther and J. Wendland\*

Junior Research Group: Growth Control of Fungal Pathogens, Hans-Knöll Institute for Natural Products  
Research and Department of Microbiology, Friedrich-Schiller University, Jena D-07745, Germany

Received 26 July 2003/Accepted 1 December 2003

**The yeast-to-hypha transition is a key feature in the cell biology of the dimorphic human fungal pathogen *Candida albicans*. Reorganization of the actin cytoskeleton is required for this dimorphic switch in *Candida*. We show that *C. albicans* *WAL1* mutants with both copies of the Wiskott-Aldrich syndrome protein (WASP) homolog deleted do not form hyphae under all inducing conditions tested. Growth of the wild-type and *wal1* mutant strains was monitored by in vivo time-lapse microscopy both during yeast-like growth and under hypha-inducing conditions. Isotropic bud growth produced round *wal1* cells and unusual mother cell growth. Defects in the organization of the actin cytoskeleton resulted in the random localization of actin patches. Furthermore, *wal1* cells exhibited defects in the endocytosis of the lipophilic dye FM4-64, contained increased numbers of vacuoles compared to the wild type, and showed defects in bud site selection. Under hypha-inducing conditions *wal1* cells were able to initiate polarized morphogenesis, which, however, resulted in the formation of pseudohyphal cells. Green fluorescent protein (GFP)-tagged Wal1p showed patch-like localization in emerging daughter cells during the yeast growth phase and at the hyphal tips under hypha-inducing conditions. Wal1p-GFP localization largely overlapped with that of actin. Our results demonstrate that Wal1p is required for the organization of the actin cytoskeleton and hyphal morphogenesis in *C. albicans* as well as for endocytosis and vacuole morphology.**

Polarized cell growth is a basic feature of the morphogenesis of a cell. Highly elongated cell growth can be found in specialized cells such as neurites, plant root hairs, and pollen tubes but is most prominent in fungal hyphae (10, 21, 45). Fungi grow either in a yeast-like or filamentous manner. Dimorphic fungi are able to switch between these two growth modes. A dimorphic transition occurs in a variety of pathogenic fungi such as the maize pathogen *Ustilago maydis* and the human pathogen *Candida albicans* (6, 32). In *C. albicans* the ability to initiate hyphal growth is associated with its virulence (27). Polarized growth in ascomycetous fungi is dependent on the actin cytoskeleton, whereas microtubules are not required to initiate hyphal extensions (19, 52). Rho protein modules are central regulators for the organization of the actin cytoskeleton (12). In fungal cells these modules determine the establishment of cell polarity and the maintenance of hyphal growth (12, 48). The actin cytoskeleton can be divided into two components: actin cables and cortical actin patches. Actin cables in *Saccharomyces cerevisiae* are positioned in a mother-daughter axis and serve as tracks for the transport of secretory vesicles delivering plasma membrane and cell wall compounds to sites of growth (37). The yeast formin Bni1p plays a key role in the Arp2/3-independent assembly of actin cables (14, 15, 38, 40). Cortical actin patches are positioned at sites of exo- and endocytosis. They localize to sites of polarized growth, for exam-

ple, to the growing bud and to hyphal tips in *C. albicans* and to the hyphal tips in filamentous fungi (for reviews, see references 37 and 45). However, the role of cortical actin patches during polarized growth or hypha formation in both *S. cerevisiae* and *C. albicans* has been questioned (5, 36). In *S. cerevisiae* the Arp2/3 complex was shown to be required for endocytosis and the assembly of actin patches (30, 49). The Arp2/3 complex can be activated by the *S. cerevisiae* homolog of the human Wiskott-Aldrich Syndrome protein (WASP), encoded by the *LAS17/BEE1* gene (9, 50). In our efforts to understand signaling routes to the actin cytoskeleton, we identified the *C. albicans* WASP homolog and characterized its role for polarized morphogenesis and hyphal growth in *C. albicans*. Mutant *wal1* cells were not able to produce hyphae under all conditions tested. Surprisingly, even though *wal1* yeast cells grew isotropically, initiation of polarized morphogenesis occurred under hypha-inducing conditions and resulted in the formation of elongated, pseudohyphal cells. In addition to the defects in the organization of the actin cytoskeleton, *wal1* mutants showed defects in endocytosis and vacuolar morphology.

## MATERIALS AND METHODS

**Strains and media.** The *C. albicans* and *S. cerevisiae* strains used in this study are listed in Table 1. Growth media and standard procedures were described previously (44). Maltose (2%) was supplied as the sole carbon source to induce expression from the *MAL2* promoter.

**Construction of disruption cassettes.** The *C. albicans* WASP homolog *WAL1* was identified in the genomic sequence (<http://www-sequence.stanford.edu/group/candida>) and contains an open reading frame (ORF) of 2,142 bp. Based on this sequence, two primers were designed (primer sequences are listed in Table 2), KpnI-WAL1 (no. 556) and XbaI-WAL1 (no. 557), to amplify a 1,551-bp fragment from genomic *C. albicans* DNA containing the 5' end of the *WAL1* ORF. This fragment was cloned into pBluescript SK(+) using the terminally attached restriction sites, generating pSK-5'WAL1. The sequence of the

\* Corresponding author. Mailing address: Department of Mikrobiologie, Hans-Knoell Institute for Natural Products Research e.V. and Friedrich-Schiller-University, Hans-Knoell Str.2/Winzerlaer Str. 10, D-07745 Jena, Germany. Phone: 49-3641-65-7639. Fax: 49-3641-65-7633. E-mail: juergen.wendland@uni-jena.de.

<sup>†</sup> Supplemental material for this article may be found at <http://ec.asm.org/>.

TABLE 1. Strains used in this study

Strain	Genotype	Reference
<i>C. albicans</i>		
SC5314	Wild type	15a
BWP17	<i>ura3::ximm34/ura3::ximm34 his1::hisG/his1::hisG/arg4::hisG/arg4/hisG</i>	48a
CAT4	<i>WAL1/wal1::HIS1</i> in BWP17	This study
CAT5	<i>WAL1/wal1::URA3</i> in BWP17	This study
CAT6	<i>wal1::URA3/wal1::HIS1</i> in BWP17	This study
CAT10	<i>wal1::MAL2p-WAL1:HIS1/wal1::URA3</i> in BWP17	This study
CAT19	<i>WAL1-GFP:HIS1/WAL1</i> in BWP17	This study
CAT20	<i>WAL1-GFP:URA3/WAL1</i> in BWP17	This study
CAT21	<i>WAL1-GFP:HIS1/wal1::URA3</i> based on CAT19	This study
<i>S. cerevisiae</i>		
RLY157	<i>MATa ura3-52 his3-Δ200 leu2-3,112 lys2-801Dbee1::LEU2</i>	25
YMW171K	<i>MATa las17::kanMX4 ade2-101 his3-200 leu2-1 lys2-801 trp1-63 ura3-52</i>	28
RH4207	<i>MATa las17::kanMX4 bar1::LYS2 ade2-101 his3-200 leu2-1 trp1-63 ura3-52</i>	28

insert was verified (MWG-Biotech, Ebersberg, Germany). Cleavage of this plasmid by HincII and ClaI resulted in the removal of an internal 460-bp fragment of the insert, which was replaced by the selectable marker genes *URA3* and *HIS1*, respectively, which were excised from pFA-URA3 and pFA-HIS1 (16) with PvuII-ClaI and HincII-ClaI, respectively. In this way, plasmids pSK-Cawall::URA3 and pSK-Cawall::HIS1 were generated that carry disruption cassettes in which the selectable marker genes are flanked by 235 bp at the 5' end and 821 bp at the 3' end with regions from the *WAL1* target locus. Both disruption cassettes were released from the plasmid backbone prior to transformation by cleavage with XbaI and KpnI. With the development of the pFA vector series (16), further genetic manipulations were carried out using PCR-based approaches.

**Construction of *MAL2* promoter-*WAL1* ORF fusion.** To place *WAL1* under control of the regulatable *MAL2* promoter, a PCR-based approach was applied. To this end, a cassette was amplified from plasmid pFA-HIS1-MAL2p (16) with primers 676 and 677. With these primers, 100 bp of sequence with homology to two positions at the 5' end of the *WAL1* gene was added to the cassette. This PCR fragment was used to transform a heterozygous *WAL1/wal1::URA3* strain, placing the only copy of *WAL1* under regulated expression.

**Construction of the *WAL1-GFP* fusion.** To generate a *WAL1-GFP* fusion, a similar PCR-based approach was applied. Transformation cassettes were amplified from pFA-GFP-URA3 and pFA-GFP-HIS1 using primers 956 and 957, which, again, added 100 bp of flanking homology region to the FA cassettes (the green fluorescent protein [GFP] variant used in these constructs was derived from plasmids described previously [8, 33]). The amplified PCR fragments were transformed into strain BWP17, generating strains CAT19 and CAT20, in which one allele of *WAL1* was tagged with GFP while the other allele remained wild type. Using CAT19 in another PCR-targeting experiment, the remaining wild-type copy of *WAL1* was deleted with a disruption cassette generated with primers 676 and 957 using pFA-URA3 as the template. The resulting strain, CAT21, carries only the GFP-tagged *WAL1* allele under its endogenous promoter, thus producing only Wall protein tagged with the GFP moiety. All three GFP-tagged strains revealed similar GFP signals. However, CAT21 produced brighter GFP signals than did the heterozygous strains.

**Transformation of *C. albicans*.** The lithium acetate procedure was used as described previously (44). Basic features of this protocol include an overnight incubation with lithium acetate and a subsequent heat shock for 15 min at 44°C. Correct gene targeting was verified by PCR analysis of the transformants. Locus- and marker-specific primers were as listed in Table 2.

**Hyphal induction of *C. albicans*.** Different protocols were used to induce hyphal formation in *C. albicans* strains at 37°C. Hyphal induction occurred most vigorously in minimal medium containing 10 to 20% serum (calf serum; Sigma). Alternatively, hyphal induction was carried out in spider medium (26). Plates inoculated with different strains were incubated for 4 to 7 days before being photographed. Hyphal induction was also tested in liquid minimal media.

**Time-lapse microscopy.** Strains were pregrown in either complete or minimal medium, harvested, washed, and resuspended in sterile water. Small aliquots of cells were applied on deep-well slides prepared as described previously (20). It was of utmost importance to provide sufficient oxygen supply to the cells within the medium to support the growth of *C. albicans*. To achieve this, the medium was vigorously vortexed prior to the preparation of microscopy slides, using a FVL2400 Combi-Spin vortex (Peqlab, Erlangen, Germany). Minimal medium or

full medium (supplemented with 10 to 20% serum for hyphal induction) was diluted 1:1 with water-agarose containing 3.4% agarose. Temperature control was achieved with a heat stage (built at the Biozentrum Basel and generously provided by P. Philippson) which was mounted on the microscope table and heated with a water bath. All microscopy was done on a motorized Zeiss Axio-plan II imaging microscope. Images were acquired using Metamorph 4.6 software (Universal Imaging Corp.) and a digital imaging system (MicroMax1024; Princeton Instruments). Images were collected into stacks. Stacks containing bright-field/differential interference contrast (DIC) images were processed separately from images displaying GFP or vacuolar fluorescence. The stacks were then combined by using overlay tools of the Metamorph software and processed as videoclips with a frame rate of 10 images/s.

**Staining procedures.** For actin staining, early-log-phase cells were fixed with 3.7% formaldehyde. Fixation and incubation with rhodamine-phalloidin were performed essentially as described previously (36). Chitin staining was done by directly adding calcofluor (1 μl of a 1-mg/ml stock) to 100 μl of cell suspension, incubating for 15 min, and washing. Vacuolar staining was done using the lipophilic dye FM4-64 (43). For the analysis of vacuolar morphology, overnight cultures grown in YPD were used. Cells were incubated with FM4-64 (0.2 μg/ml) for 30 min at 30°C and then photographed. For FM4-64 time-lapse microscopy, exponentially grown cells of the wild type and the *wal1* mutant strain were placed on precooled microscope slides containing medium made of equal amounts of YPD and 3.4% water-containing agarose. GFP-images were obtained from early-log-phase cells grown in 0.25 × YPD that were washed once with water and resuspended in water. For GFP and actin colabeling, cells were fixed and stained with rhodamine-phalloidin as described above; the GFP signal was obtained using a narrow-band GFP filter set which excludes the actin signal monitored by a tetramethylrhodamine-5-isothiocyanate (TRITC) filter set. Other images were acquired using the appropriate filter sets (Chroma Technology).

**Heterologous complementation.** The *C. albicans* *WAL1* ORF was amplified from a plasmid library (kindly provided by J. Ernst) by using primers 975 and 976. The resulting PCR product carried terminal flanking homology regions to the *Ashbya gossypii* *TEF1* promoter and *TEF1* terminator. This PCR product was cotransformed into an *S. cerevisiae* *bee1/las17* strain together with NruI-linearized plasmid pRS415-kanMX carrying the KanMX selection marker (as described in reference 46). Transformant colonies appeared after 2 days of growth at 30°C on selective plates lacking leucine. Digestion of pRS415-kanMX with NruI cleaves a unique restriction site within the *kan* ORF. The *S. cerevisiae* in vivo recombination machinery was used to recombine the plasmid and PCR fragment, thus generating a new plasmid, pXL-CaWAL1, in which the *WAL1* ORF is placed under control of the *A. gossypii* *TEF* promoter (this promoter is functional in *S. cerevisiae*). Transformant colonies were restreaked on new selective plates and incubated at 37°C, the restrictive temperature for *bee1/las17* strains. Transformants that continued to grow were selected, and plasmid DNA was isolated from these transformants and amplified in *Escherichia coli*. Correct fusion that generated pXL-CaWAL1 was verified by PCR, restriction, and sequence analyses. Retransformation of pXL-WAL1 into *S. cerevisiae* *bee1/las17* cells revealed that heterologous complementation by pXL-CaWAL1 was dependent on a period (6 h) of growth at 30°C prior to the shift to 37°C. This preincubation was not required when using a plasmid carrying the *BEE1/LAS17*

gene, suggesting that even on overexpression of *WAL1* with the *AgTEF1* promoter, *Wal1p* is not fully competent to take over the position of *Bee1p/Las17p*.

### RESULTS

**The unique gene *WAL1* encodes the *C. albicans* WASP homolog.** The *C. albicans* genome database at Stanford University was searched for sequences homologous to the human WASP. A single ORF was found which corresponds to orf19.6598.prot. This gene was designated *WAL1* (for ‘‘Wiskott-Aldrich syndrome-like’’). Its ORF is 2,139 bp and encodes a 713-amino-acid protein with an apparent molecular mass of 76.9 kDa. *Wal1p* shows the highest sequence identity at the amino acid level to *S. cerevisiae* *Las17p/Bee1p* (37.6%) and *Schizosaccharomyces pombe* *Wsp1p* (27.7%). WASP family members contain specific functional domains including an amino-terminal WH1 domain and the carboxy-terminal WH2-C-A domain. Within these domains, conservation is particularly high, reaching 75% for WH1 domains and 60% for the acidic C terminus (Fig. 1). In contrast, the internal proline-rich region is rather divergent. Sequence analysis of *Wal1p* and all other fungal WASPs identified so far indicated that they do not contain *Cdc42/Rac* interactive binding (CRIB) motifs. Furthermore, heterologous complementation of the *S. cerevisiae* *bee1/las17* temperature-sensitive mutant phenotype with *WAL1* indicated that *WAL1* encodes the functional homologue of *Bee1p/Las17p* (for details, see Materials and Methods).

***WAL1* is not essential for cell viability in *C. albicans*.** To be able to study the function of *WAL1* in *C. albicans*, homozygous mutant strains were generated from independent heterozygous strains. Strain BWP17 was chosen as the progenitor strain since its auxotrophies enabled the sequential disruption of both alleles with the *HIS1* and *URA3* marker genes (for details, see Materials and Methods).

*wal1::HIS1/wal1::URA3* mutant strains were phenotypically identical, indicating that correct gene targeting had occurred as verified by analytical PCR. Additionally, starting from a heterozygous mutant strain (*WAL1/wal1::URA3*), the remaining copy of *WAL1* was placed under the control of the regulatable *MAL2* promoter, which is repressed in a glucose-containing regimen but can be induced by growth on maltose (see Materials and Methods). This strain (*wal1::MAL2p-WAL1::HIS1/wal1::URA3*) behaved phenotypically like the wild-type strain when grown on maltose but showed the WASP mutant phenotypes described below when grown on glucose. Thus, the deletion of *WAL1* is solely responsible for the observed morphological phenotypes of the *wal1* strains. Strains bearing disruptions in the *WAL1* genes or strains in which the expression of *WAL1* is downregulated are viable, demonstrating that *C. albicans* *WAL1* is not an essential gene.

The *S. cerevisiae* WASP mutant *bee1/las17* is temperature sensitive and does not grow at temperatures above 34°C (25). In contrast, growth of the *C. albicans* WASP mutant either in liquid culture or on solid-medium plates was not inhibited in the temperature range tested (20 to 42°C) (data not shown).

***Wal1p* is required for polarized cell growth during the yeast growth phase.** We used digital in vivo microscopy to monitor and compare growth of the wild type (Fig. 2A) with growth of a *wal1* strain (Fig. 2B) (see Movies S1 to S3 in the supplemental material, which also includes a movie of the heterozygous

TABLE 2. Oligonucleotide primers used in this study

Primer no.	Primer name	Sequence <sup>a</sup>
392	XFP-primer	CATAACCTTGGGGCAITGGCACACTC
397	TEF-term	CTGGGAGATGATGTGGAGGC
511	TEF-prom	AGGATTTCACAGGTTCTTC
549	G4- <i>CaWAL1</i>	CATATCAACTTAATAATTTGGG
555	G1- <i>CaWAL1</i>	CCTTATATTCATCCATCC
556	Kpnl- <i>WAL1</i>	ItcaggtaaccGGATAATGATGATGATCAACTGTAAGTTC
557	XbaI- <i>WAL1</i>	ataatctagcCAATGAATGATTTTAAACCACTC
577	G1- <i>WAL1</i>	CCAAATGAATCTATTTTAAACCACTC
599	U3	GGAGTTGGATTAGATGATTAAGAAGTGATGG
600	U2	GTGTTACGAATCAATGGCACTACAGC
601	H2	CAACGAAATGGCTCCCTCCATCCACAG
602	H3	GGACGGAATTTGAAGAAGCTGGTGGCAACCG
606	S1- <i>CaWAL1</i>	GAATAACTTTGAAATCACTTCAATAATATTTTCTTTCTTTCTTCTCTCCCTCCCTCGGGGGAATACTGAGTGAAGTGAGTGGTGAAGTGA
676	S1- <i>CaWAL1</i>	GTCGGgaaactctagctacgcgactgctc
677	S1- <i>MAL2p-WAL1</i>	ATATTAATCGAGCCACCCTGGTGGCATCGATTATTTATTTGTTGGCTTTTGGAAATAGCCCGTTTAACCTTTTCTTATCTTTGAGTAGTTAATATCCCATg
720	G1- <i>CaWAL1-GFP</i>	tagtgaattatgtaaacac
742	G4- <i>MAL2-WAL1</i>	ccggaaatcggctaaatcctggtggcggaggaagaatttc
956	S1- <i>CaWAL1-GFP</i>	CGTTG-AGCAGTAAATTCACATCC
957	S2- <i>CaWAL1</i>	AGCCCGATGCACCCTGCTACTTTAGCCCGATGCATTAAGCTTTCGCTTGAATTAAGAGGAAAGAAAAGTTGGCTCAAAAGTGAATGAAGAAGAT
975	X11- <i>CaWAL1</i>	GATGATTTGGggggcgcgagctgcttc
976	X12- <i>CaWAL1</i>	GTTACTTCATCTTTAATAATTTATTTATCTTGATTGAATATCCGAAAACATTC AACATTTCATTCACCTCGGCACACTATCCCTTAATTTTTCGTAATTTTATTG
		Gtccgatalcatcagaaatccag
		TCTTTGCTAGGATACAGTTCCTCAACATCCGAACATTAACCAACCcaggggatacttaactcaagataag
		ATGACCAAGTTCTTGGAAAACAAGAAATCTTTTATTTGTCAGTACTGATthaccatcaatcctctcctcaatc

<sup>a</sup> Capital letters correspond to *C. albicans* genomic DNA. Bold capital letters correspond to the *A. gossypii* *TEF* promoter or *TEF* terminator. Italic capital letters correspond to GFP. Lowercase letters correspond to 5'-terminal regions of primers containing restriction sites (bold) or to 3'-terminal annealing regions for the amplification of transformation cassettes. All sequences are written from 5' to 3'.

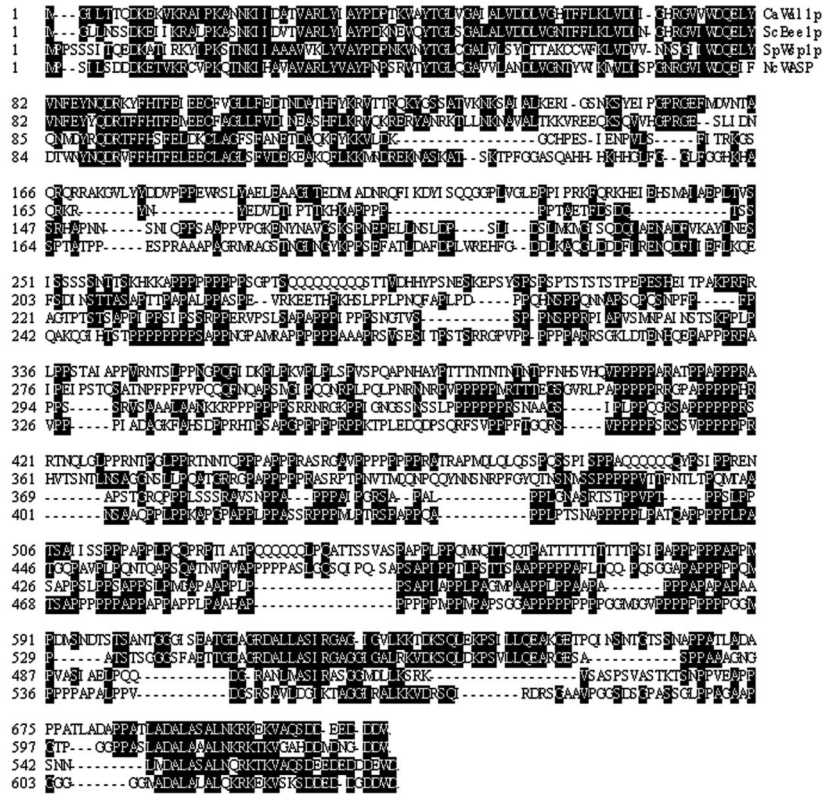


FIG. 1. Alignment of fungal Wasp homologs. Amino acids corresponding to a majority of aligned sequences are shaded. Accession numbers: *C. albicans* Wal1p, orf19.6598.prot (<http://www-sequence.stanford.edu/group/candida/index.html>), *S. cerevisiae* Bee1p/Las17p, NP01482; *S. pombe* Wsp1p, NP594758; *Neurospora crassa* Wasp, NCU07438.1 (<http://www-genome.wi.mit.edu/annotation/fungi/neurospora/>).

mutant strain). With our setup, we were able to monitor the growth of the strains over a period of approximately 10 h (sometimes up to 15 h). In contrast to similar studies with *S. cerevisiae* cells, it was essential to provide sufficient oxygen when growing *C. albicans* cells under these conditions (see Materials and Methods). We analyzed the *wal1* mutant strains, their BWP17 progenitor strain, and the wild-type strain (SC5314) for growth defects during the yeast stage. *WAL1*<sup>+</sup> cells were ellipsoidal. In contrast, *wal1* cells were found to be round and of heterogeneous size, with several cells clumping together. To quantify the cell morphology defect of *wal1* cells, we measured the lengths and widths of *WAL1* and *wal1* cells (Fig. 3A). Cell indices (length/width) of wild-type, BWP17, and heterozygous mutant strains were 1.3, corresponding to the ellipsoidal cell shape. This indicates that heterozygosity of *WAL1* did not result in morphological defects and that a single copy of *WAL1* is sufficient for wild-type-like growth. In contrast, the cell index of the *wal1* strain was 1.1, representing an almost spherical cell shape. The ability to form new buds was not affected in *wal1* cells. In the wild-type strain, bud emergence was followed by a period of polarized growth (Fig. 3B). *wal1* cells, however, quickly began to grow in an isotropic manner, which resulted in a decrease of the polarized-growth rate (Fig. 3B). Due to the extended duration of our time-lapse recordings, we were able to observe several consecutive cell divisions of wild-type and *wal1* cells. The time required for two consecutive bud emergence events of a single cell was used

calculate the average time of a cell cycle (Fig. 3C). Growth delays in the mutant strains were at least in part attributable to the remaining auxotrophies, since the heterozygous *WAL1/wal1::HIS1* strain grew more slowly than a heterozygous *WAL1/wal1::URA3* strain, which is a general feature that has been observed in other mutant strains as well (our unpublished results). In line with this observation, both of the heterozygous mutant strains required more time to complete a cell cycle than the homozygous mutant strain which carries only the *arg4* auxotrophy. The cell cycle times observed in the in vivo time-lapse recordings were found to be similar to the growth rates in liquid culture (data not shown). Cells of the *wal1* mutant appeared to be of heterogeneous size. To analyze this in more detail, we monitored cell size changes of single cells over time (Fig. 3D). We found that wild-type mother cells only marginally increased in cell volume. In contrast, the volume of *wal1* mother cells increased more than 50% during the 6-h observation period, which corresponds to about four cell cycles. Another difference between the wild-type and *wal1* occurred during the detachment of mother and daughter cells, which in the wild-type resulted in a torsion of the daughter cell out of the mother-daughter cell axis whereas *wal1* mutant cells only rarely showed such an obvious displacement (Movies S1 and S3 in the supplemental material). Mutant *wal1* cells adhered and relocated as cell clumps, indicating a defect in cell separation. This led to the formation of cell heaps not observed in the wild type or in the heterozygous mutant strains, where all cells

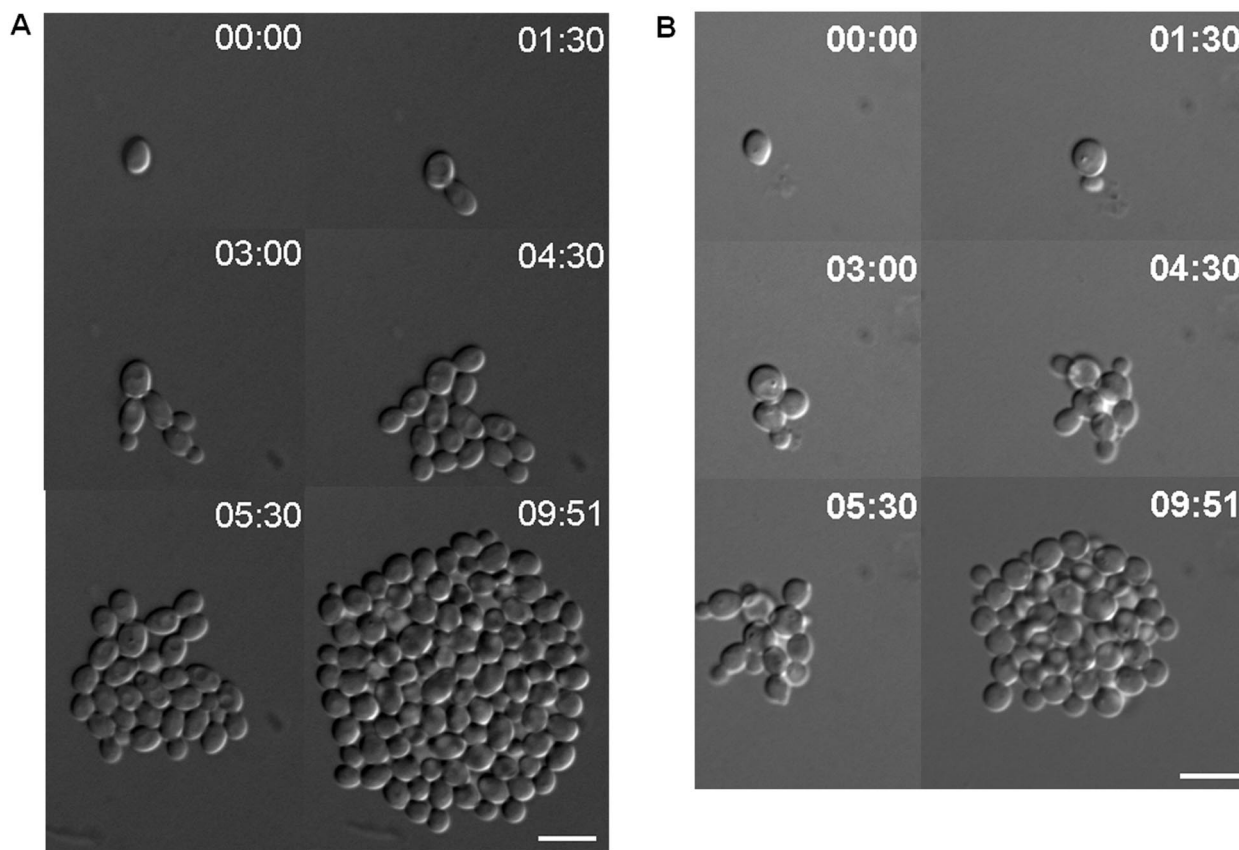


FIG. 2. In vivo time-lapse analysis of yeast cell growth of wild-type and *wall* mutant strains. Representative frames of movies of the wild-type (A) and *wall* (B) cells are shown at the same time points. Note the cell shape differences between wild-type (ellipsoidal) and *wall* (round) cells. The small delay in cell cycle time of the *wall* strain compared to the wild-type amounts adds up to one cell cycle interval after 10 h, resulting in different cell numbers. Bars, 10  $\mu$ m. Time is given as hh:min.

remained in the focal plane during the time-lapse recordings, indicating that effective displacement had occurred. Cell clumps were also found when growing *wall* in liquid culture. Cell aggregates could be resolved mechanically, indicating that cytokinesis and separation of mother and daughter cytoplasm had occurred.

**Wallp determines polarity development.** In *S. cerevisiae*, the actin cytoskeleton is involved in establishing the bipolar budding pattern of diploid cells, and mutations in a number of genes including *BEE1/LAS17* affect the budding pattern (2, 25, 51). Therefore, we examined the distribution of bud scars in *wall* and wild-type cells. Cells of the *wall* strain with three or more bud scars showed a high degree of randomized bud-site selection whereas the wildtype displayed regular (bi)polar budding (Fig. 4; Table 3). Determination of a new bud site is an initial step that polarizes the actin cytoskeleton toward the incipient bud site in the wild type. We therefore examined the distribution and positioning of cortical actin patches in *wall* in comparison to wild-type cells (Fig. 5). In wild-type cells, actin cortical patches localized within the bud at an early growth stage, then redistributed between mother and daughter cell during the isotropic growth phase of the bud, and finally localized to the bud neck to prepare for cytokinesis (Fig. 5A). In contrast, in *wall* cells, cortical actin patches were randomly distributed in mother and daughter cells throughout the cell

cycle (Fig. 5B). Depolarization of cortical actin patches therefore accompanies isotropic growth, misplaced growth of mother cells, and defects in bud site selection of mutant cells.

**Mutant *wall* cells exhibit defects in endocytosis and in vacuolar morphology.** Defects in vacuolar morphology resulting in fragmented vacuoles were observed in *S. cerevisiae* in a certain allele of *BEE1/LAS17*, *las17-16*, which contains a C-terminal deletion of 21 aa that inactivates the Arp2/3-complex activation domain (11). To determine defects in vacuolar morphology in the *wall* strain, we stained *Candida* wild-type and *wall* cells using the lipophilic dye FM4-64 (Table 4). Our results clearly show that in contrast to wild-type cells, which contain one or two large vacuoles, *wall* strains contain a large number of cells with multiple vacuoles and only few cells with just one large vacuole (Table 4).

Furthermore, in *S. cerevisiae* the cortical actin cytoskeleton and Bee1p/Las17p are involved in endocytosis (28). Therefore, we examined endocytosis in *Candida* wild-type and *wall* cells by monitoring the uptake of FM4-64 in vivo using time-lapse microscopy (Fig. 6; Movie S4 in the supplemental material). Wild-type cells rapidly incorporated the dye, which resulted in staining of endosomes that moved around in the cytoplasm after 4 min (Fig. 6). Later (beginning after approximately 30 min in the time-lapse sequence), vacuoles of the wild type were stained, indicating efficient transport of the dye to the vacuole

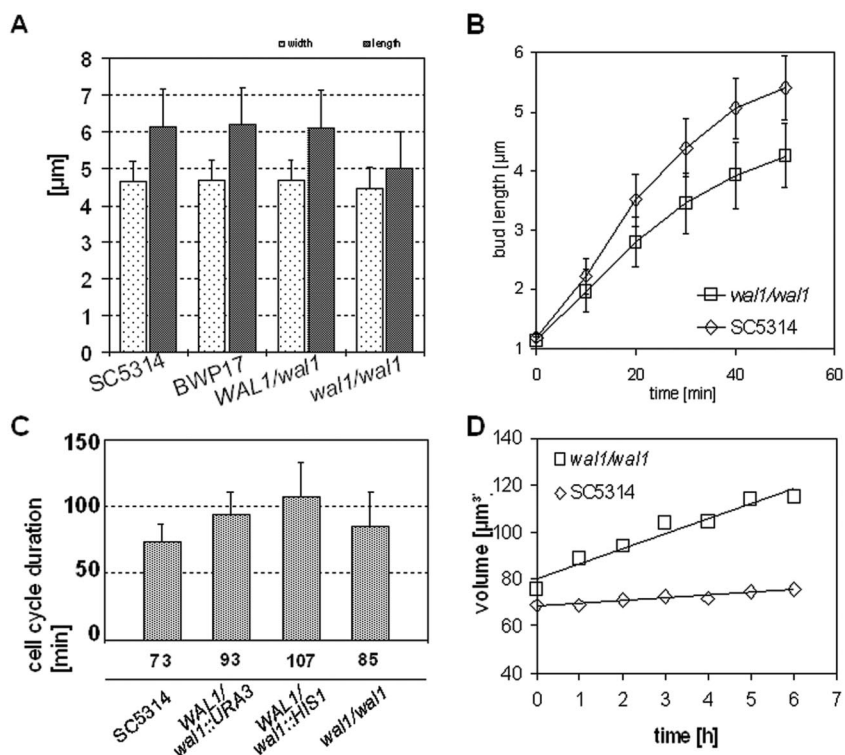


FIG. 3. Analysis of yeast cell morphology of the *wal1* mutant. (A) Cell sizes (length and width) of yeast cells of the indicated strains that were grown to early log phase in YPD were determined. The average of 500 cells per strain (measured using Metamorph 4.6. software) is displayed. (B) Comparison of bud growth of wild-type and *wal1* daughter cells. Using time-lapse microscopy, bud extension was measured for 60 min starting once a bud reached a size of  $>1 \mu\text{m}$ . For each strain, 18 cells were measured. The calculated growth rates for the wild type and the *wal1* strain were 5.8 and 4.2  $\mu\text{m}/\text{h}$ , respectively. (C) Cell cycle duration was measured by analysis of time-lapse data. One cell cycle was measured as the time required from one bud emergence of a cell to its next budding event. For each strain, 24 to 40 cells were analyzed. Note the different effect on cell cycle duration in heterozygous strains carrying either *ura3* or *his1* auxotrophies. (D) Analysis of mother cell growth of the wild type and the *wal1* mutant. Time-lapse recordings of wild-type and *wal1* strains grown at 26°C were analyzed. At hourly intervals, cell sizes (length and width) of wild-type mother cells ( $n = 7$ ) and *wal1* cells ( $n = 7$ ) were measured. Based on these measurements, volumes of cells were calculated. For *wal1* cells, a spherical form was assumed based on the cell indices (Fig. 3A) and volume was calculated from  $V = 1/6 \times \pi \times d^3$ . Wild-type cells have an approximately ellipsoidal shape. Their volume was calculated as  $V = \pi \times b^2 \times 4/3 \times a$ , where  $a$  is half the length of the cell and  $b$  is half the width of the cell.

(Fig. 6). Cells of the *wal1* mutant, in contrast, required a prolonged time to internalize the dye (Fig. 6). Staining of endosomes was not observed in *wal1* cells. Vacuolar staining appeared with a long delay compared to the wild type and was found to be much weaker than in the wild type (Fig. 6).

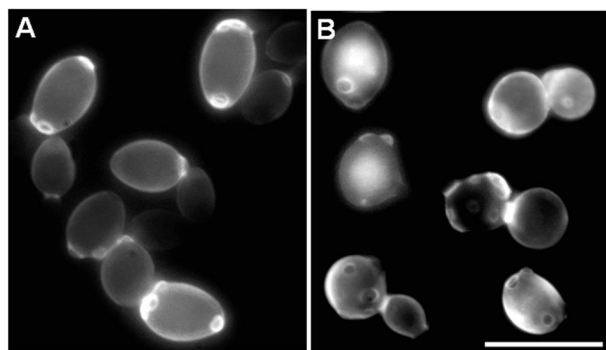


FIG. 4. Bud-site selection defects in *wal1* cells. The wild-type (A) and *wal1* mutant (B) strains were grown overnight in YPD at 30°C. The cells were stained with Calcofluor white, washed, and observed using fluorescence microscopy. Bar, 10  $\mu\text{m}$ .

**Wal1p is required for polarized hyphal growth in *C. albicans*.** In contrast to *S. cerevisiae*, *C. albicans* is a dimorphic fungus that is capable of forming true hyphae. *WAL1*<sup>+</sup> and *wal1*<sup>-</sup> cells were induced to form hyphae under different inducing conditions (see Materials and Methods). Cells of the wild-type and heterozygous *WAL1/wal1* strains initiated the formation of hyphae when grown on spider medium or on medium supplemented with serum. In contrast, hyphal growth was abolished in the *wal1* mutant strain under these conditions (Fig. 7A). Hyphal growth resulted in wrinkled colonies (indicative of colonies containing hyphae and yeast cells), whereas yeast-like growth gave rise to shiny and smooth colonies. Hyphal growth was induced in the heterozygous mutant strain, in which the remaining copy of *WAL1* was placed under the control of the regulatable *MAL2* promoter when grown on serum-containing medium supplemented with maltose as the sole carbon source (Fig. 7B). These results demonstrate that Wal1p is required for hyphal growth in *C. albicans*. Microscopic examination indicated, however, that cell shape changes occurred in *wal1* cells induced for hypha formation. Therefore, time-lapse analyses were used to monitor the growth of the wild-type and *wal1* mutant strains under serum-inducing con-

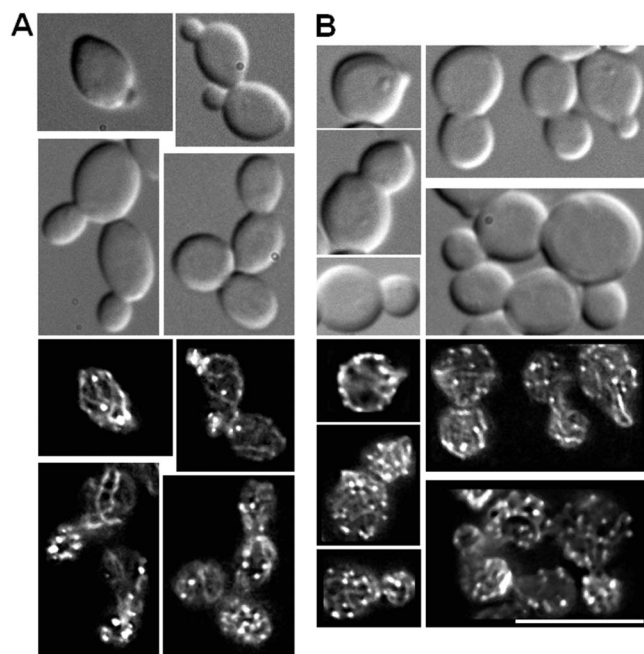
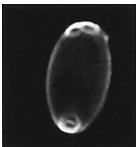
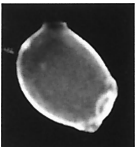
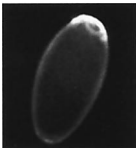
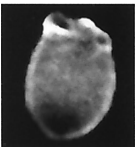
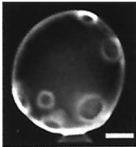



FIG. 5. Distribution of cortical actin patches in wild-type and *wall* yeast cells. Logarithmically growing cells of the wild-type (A) and *wall* mutant (B) strains were fixed twice for 1 h, washed, and stained overnight in rhodamine-phalloidin. Cells were imaged using DIC and fluorescence microscopy settings. Representative images of different cell cycle phases are shown, indicating the polarized distribution of cortical actin patches in the wild type and random localization of patches in the mutant. Bar, 10  $\mu\text{m}$ .

ditions (Fig. 8A and B; Movies S5 and S6 in the supplemental material). In the wild type, hyphal formation occurred almost immediately on induction. Hyphae grew out with an extension rate of approximately 20  $\mu\text{m}/\text{h}$ . These hyphae maintained hyphal growth and formed lateral branches. Interestingly, in the center of the mycelium, yeast cells were produced after 5 to 6 h under inducing conditions (Fig. 8A; Movie S5 in the supplemental material). In contrast, *wall* yeast cells initially responded to hyphal induction with polarized morphogenesis (Table 5). Polarized growth occurred with an extension rate of approximately 15  $\mu\text{m}/\text{h}$  (Fig. 8B; Movie S6 in the supplemental material). Clear differences between hyphal and pseudohyphal cells can be seen at sites of septation. Whereas true hyphae formed septa that appeared as cross-walls not changing the diameter of the hyphal tube, pseudohyphal cells showed constrictions at septal sites (Fig. 8C and D; arrows). Thus, the septum position in the *wall* mutant strain indicates that pseudohyphal cells were formed. In our experiments, 69% of wild-type cells responded to hypha-inducing conditions (10% serum) with germ tube formation, a few cells developed pseudohyphae, and a minor fraction did not respond and stayed in the yeast phase. In the same experiment, *wall* cells did not form hyphae, the majority of cells (66%) formed pseudohyphae, and one-third of the cells did not respond to the induction (Table 5).

**Wal1p exhibits a patch-like localization to sites of polarized secretion.** To determine the intracellular localization of Wal1p, we fused GFP to the 3' end of *WAL1* by using PCR-amplified

TABLE 3. Analysis of bud site selection patterns

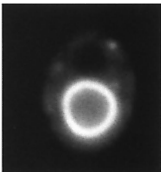
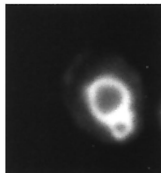

Pattern	% of SC5314 cells	Appearance	% of <i>Cawal1/wall1</i> cells	Appearance
Bipolar	52.8		29.5	
Unipolar	44.0		25.0	
Random	3.1		45.5	
No. of cells counted	159		852	

cassettes with a 100-bp homology region to the target locus. We constructed two independent strains carrying heterozygous *WAL1/WAL1-GFP* alleles. From one of these strains, CAT19, a strain was constructed that produces only GFP-tagged Wal1p (*WAL1-GFP:HIS1/wall1::URA3*) under the control of its endogenous promoter. This strain, CAT21, showed wild-type morphology, indicating that the *WAL1-GFP* construct is fully functional and suggesting that the GFP signals that were obtained reflect the correct localization pattern of Wal1p. GFP signals were similar in all strains, but the brightest signal could be obtained from CAT21, which was therefore used for localization studies presented here. We analyzed the distribution of Wal1p-GFP in both yeast cells and in hyphal cells (Fig. 9). Wal1p-GFP localized in a patch-like structure to sites of growth; it accumulated in emerging buds and at the tips of hyphae (Fig. 9). This, in part, resembles the localization of cortical actin patches, which also cluster in daughter cells and at hyphal tips (Fig. 5). In *S. cerevisiae*, localization of myc-tagged Bee1p revealed that the majority of Bee1p patches colocalize with actin patches (25). Colocalization with actin patches was also observed for other proteins, for example, for the *C. albicans* Myo5p, representing the only myosin I (36). To determine the colocalization of Wal1p with actin patches, we used double-label experiments. To this end, the actin cytoskeleton of strain CAT21 (*WAL1-GFP*) that was induced for hyphal formation was stained with rhodamine-phalloidin. Overlay of the two signals revealed that Wal1p-GFP found as patches colocalized with actin patches (Fig. 9B). Additionally, other, more disperse Wal1p-GFP signals appeared not to colocalize with actin patches.

## DISCUSSION

We chose to work on the dimorphic human fungal pathogen *C. albicans* in order to study polarized morphogenesis because

TABLE 4. Analysis of vacuolar morphology

No. of vacuoles	% of SC5314 cells	Appearance	% of <i>Cawall/wall</i> cells
1	54.9		12.3
2 or 3	42.0		36.5
4 or more	3.1		51.2
No. of cells counted	257		293

this organism is able to switch between yeast-like and hyphal growth modes under defined regimens. This dimorphism plays an important role during several stages of infection, for example, during invasion of host tissues, evasion of the cellular host immune response, and colonization of internal organs (22, 31). We have shown previously that in the filamentous fungus *A. gossypii*, Rho protein modules play a key role in the establishment of cell polarity via the Cdc42 module and during hyphal growth via the Rho3 module by regulating the organization of the actin cytoskeleton (47, 48). The regulatory role of the Cdc42 module on the architecture of the actin cytoskeleton during yeast and hyphal stages has recently been analyzed in detail in *C. albicans* (4, 17, 42). Other components that are involved in this process were found to be required for hyphal growth in *C. albicans*, such as the *SLA2* and *MYO5* (encoding a type I myosin) genes (3, 36). Signaling from Rho protein modules is transduced to the actin cytoskeleton by effector proteins (12, 45). Effectors that can regulate actin filament assembly either directly or via other protein-protein interactions are therefore of central importance for morphogenesis in *C. albicans* and may also serve as antifungal drug targets. Fungal WASPs are different from mammalian WASP in that they lack a CRIB motif. Thus, they cannot bind directly to GTP-loaded Cdc42p. Recently, it was suggested that activation of the *S. cerevisiae* WASP Bee1p/Las17p is mediated by a complex including the G-protein Rho3p, Exo70p, and Rvs167p (1, 39).

**Functions of Wall1p.** Disruption of *WAL1* caused major defects in yeast cell morphology, the organization of the cortical actin cytoskeleton, polarized growth under hypha-inducing conditions, early endocytosis, vacuolar morphology, and bud

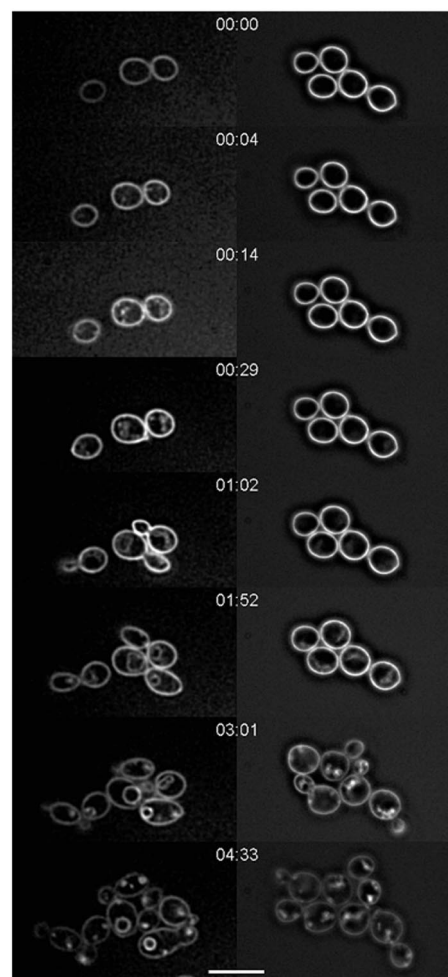


FIG. 6. In vivo time-lapse analysis of endocytosis of the lipophilic dye FM4-64. Uptake was monitored in the wild-type strain SC5314 (left column) and the *wall* mutant strain (right column). Growth of cells and setup of the microscopy slides were as described in Materials and Methods. Representative frames of both movies are shown at the same time points (hh:min). Bar, 10  $\mu$ m.

site selection. Defects of *wall* cells during yeast-like growth were similar to those observed in *S. cerevisiae* *bee1/las17* mutants (25). *S. pombe* *wsp1* mutants also exhibit defects in cell morphology, which, however, did not result in isotropic growth phases and round cells (24). In wild-type *C. albicans* yeast cells, localization of cortical actin patches follows similar polarization-depolarization events to those in *S. cerevisiae*, whereas during hyphal stages the localization of patches resembles that of true filamentous fungi (36, 45, 52). In *wall* cells, cortical actin patches were randomly positioned in mother and daughter cells during all stages of growth. This included the absence of clustered actin patches during bud emergence, suggesting that at this stage of the cell cycle, actin patches are dispensable. In contrast, the assembly of actin cables in *wall* cells appeared to be as in the wild type. At least, actin cables were found in emerging buds and appeared to localize in a mother bud axis (see, for example, the cell at the bottom right corner of Fig. 5B). Actin nucleation to form cables has recently been shown to be dependent on the formin Bni1p in *S. cerevisiae* (14, 15, 38,



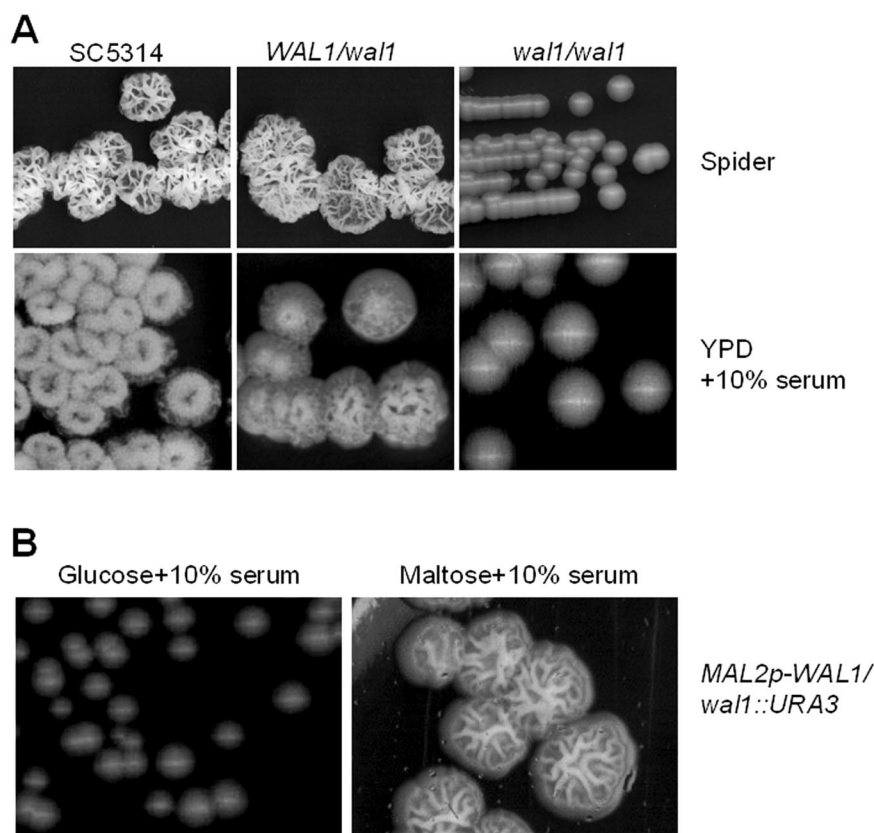


FIG. 7. Induction of hyphal growth in wild-type and mutant strains. (A) Hypha formation on solid media. Hypha formation was determined by plating the indicated strains as single cells on either Spider medium or YPD containing 10% serum. (B) Hyphal induction of strain CAT10 in which one allele of *WAL1* was deleted and the remaining copy was placed under control of the *MAL2* promoter. Plates contained 10% serum and complete medium with either glucose or maltose as the carbon source, resulting in either repressed or induced expression of *MAL2p-CaWAL1*, respectively. All plates were incubated for 4 days at 37°C prior to photography.

40). This supports a model in which bud emergence may be initiated via a pathway including Cdc42p and Bni1p whereas polarized morphogenesis is maintained by correct positioning of cortical actin patches and localized secretion, which requires a WASP homolog. In *C. albicans*, two formin homologs were identified, corresponding to the *S. cerevisiae* *BNII* and *BNR1* genes. Their function, particularly during early growth phases in *C. albicans*, is currently under investigation.

**Contribution of Wal1p to polarized morphogenesis.** Mutant *wal1* cells were unable to form hyphal filaments under all conditions tested, although these cells were able to initiate polarized morphogenesis to a limited degree on induction. Growth resulted in the formation of elongated pseudohyphal cells. In our time-lapse analyses under hypha-inducing conditions, we observed initial polarized morphogenesis in *wal1* cells that had kinetics comparable to that of the wild type. The *wal1* defect resulted in a failure to maintain polarized growth at the hyphal tip. Another hall mark of hyphal induction also failed to develop. Septation in hyphal filaments occurs as cross-walls compartmentalizing the hyphae without changing the hyphal diameter. In pseudohyphae, constrictions occur at septal sites which were also observed in *wal1* mutants. In *S. pombe* and *S. cerevisiae*, synthetic defects were observed in myosin I- and WASP-deficient strains (13, 24). This suggests a joint activity in

a larger complex since WASP provides binding sites for myosin I binding through its proline-rich region (29). Indeed, in *S. cerevisiae*, Myo3p and Myo5p were found to interact via SH3 domains with the proline-rich region of Las17p/Bee1p (13). Additionally, fungal WASPs and type I myosins share a C-terminal acidic motif for activation of the Arp2/3 complex (23, 28). This is in line with observations in *C. albicans* myosin I mutants that exhibit morphological defects similar to those described in this study for *wal1*. Cells of the *myo5* mutant (carrying deletions in the only myosin I gene) were shown to be round during yeast stages and were unable to induce hyphal growth (36). A *myo5* S366D mutation, which mimics the phosphorylation of a serine residue at the TEDS-rule site and thus activates the protein, allowed hypha formation even in the absence of an accumulation of polarized actin patches (36).

**Contribution of Wal1p to endocytosis and vacuolar morphology.** In the *S. cerevisiae* *bee1/las17* mutants, defects in endocytosis were observed and Las17p/Bee1p was found to be required for endosome and vacuole movement (7, 28, 35). Here we provide in vivo time-lapse data that clearly show similar defects in the endocytosis of the dye FM4-64 into early endosomes (Fig. 6). In addition to uptake defects, vacuolar morphology in *wal1* cells was different from that in the wild type since cells were frequently found with perturbations in the

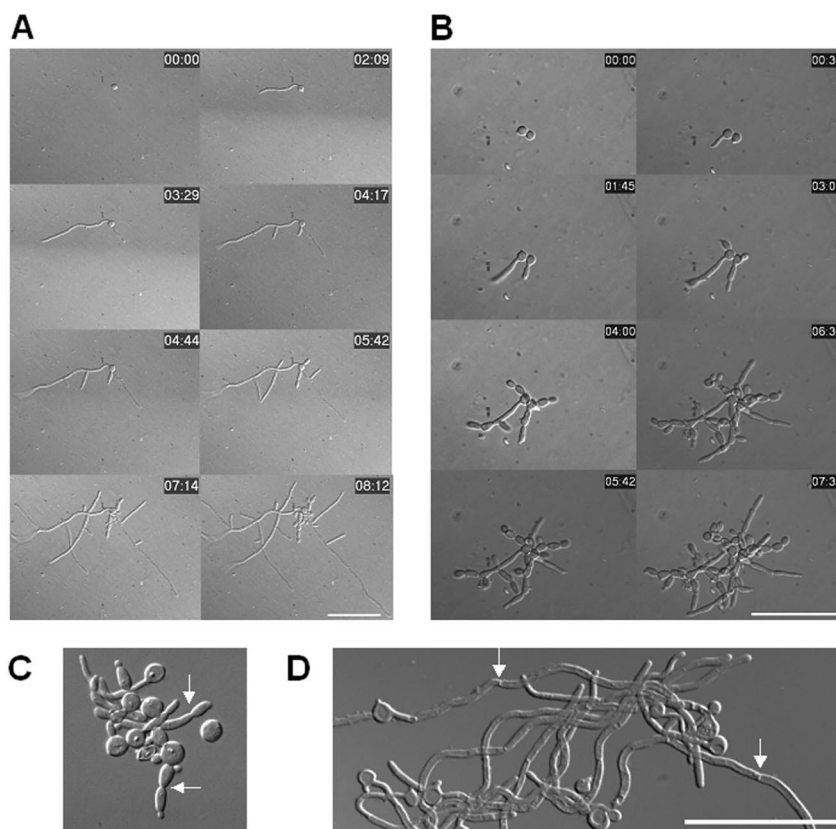
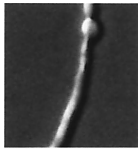

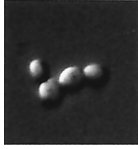


FIG. 8. In vivo time-lapse analysis of the growth of wild-type and *wal1* mutant strains under hypha-inducing conditions (A and B). Representative frames of movies of wild-type (A) and *wal1* (B) cells are shown at the indicated timepoints (hh:min). Cells were preincubated overnight in sterile water. Single cells were mounted on inducing solid media at 37°C. (C and D) Hyphal induction of strain CAT10 (*Mal2p-WAL1/wal1*) in liquid medium with glucose (C) or maltose (D) as the sole carbon source. Cells were pretreated as in panel A and incubated for 6 h prior to microscopic observation and photography. Inducing media were complete synthetic medium with 2% glucose (A to C) and 20% serum (A and B) and complete synthetic medium with 2% maltose (D) and 10% serum (C and D). Cells were incubated at 37°C. Bars, 50  $\mu$ m.

number of vacuoles (Table 4). In *S. cerevisiae*, a signal cascade starting from the Rho-type GTPase Cdc42p is required for vacuole fusion (11, 34). A genomic analysis of all viable *S. cerevisiae* mutants for mutations of homotypic vacuole fusion revealed almost 100 genes with defective vacuolar morphology (41). Among these were a number of genes required for remodeling of the actin cytoskeleton, such as *CLA4* or *BEM2* (41). The same group, showed that the *las17-16* allele produced “fragmented” vacuoles, resulting in a multivacuolar phenotype (11). These and our results suggest that fungal WASP homologues may also be involved in homotypic vacuolar fusion.

Our characterization of *WAL1* and previous results with *MYO5* suggest that both gene products are required for transport processes during endocytosis and polarized morphogenesis. These processes are essential during hyphal growth in *C. albicans* and presumably in other filamentous fungi as well. Our time-lapse analyses indicated that hyphal morphogenesis on induction of starved cells is a very fast process. Recently, it was shown that hyphal elongation occurs independently of the cell cycle in *C. albicans*. Even cells that had initiated a budding cycle were able to respond to induction cues and switched growth mode to form filaments (18). This allows us to ask new questions about hyphal growth in *Candida*, specifically whether

TABLE 5. Analysis of polarized morphogenesis

Growth form	% of SC5314 cells	Appearance	% of <i>Cawal1/wal1</i> cells
Hyphae	69.1		0.0
Pseudohyphae	13.4		66.6
Yeast	17.6		33.4
No. of cells counted	404		410

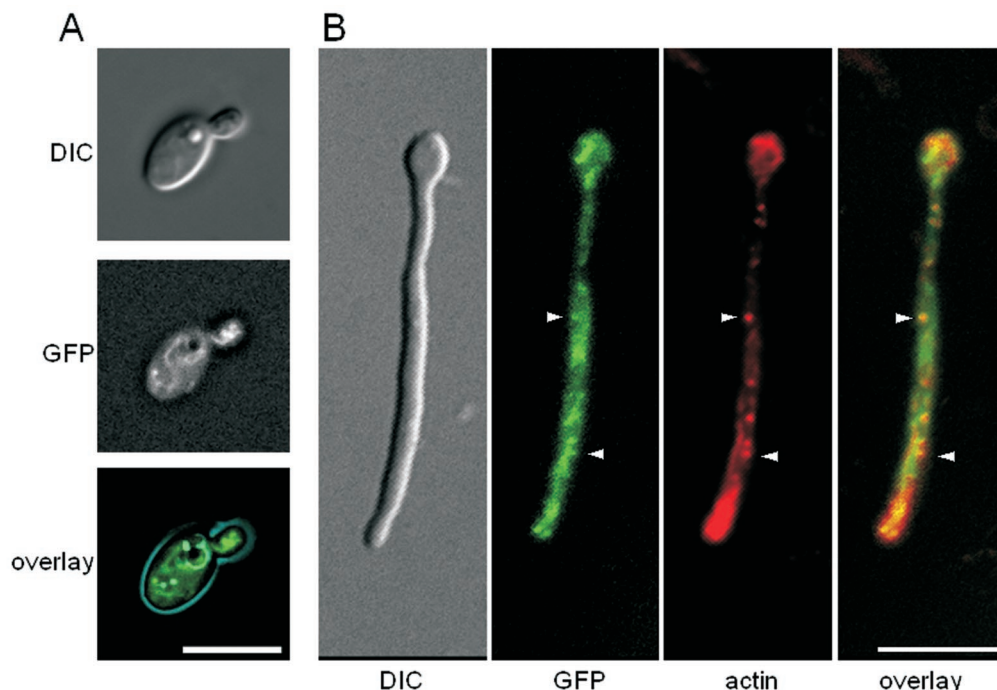


FIG. 9. Localization of Wal1p-GFP in yeast and hyphal cells. Cells of *C. albicans* strain CAT21 were used. (A) GFP fluorescence of yeast cells growing exponentially. (B) Colocalization of Wal1p-GFP and actin during the hyphal growth phase. Hyphal growth was induced by serum. Cells were fixed and stained with rhodamine-phalloidin. GFP and actin fluorescence was imaged using appropriate filter sets. Colocalization of Wal1p-GFP patches with actin patches is indicated by arrowheads. In the overlay, colocalization of GFP (green) and actin (red) results in yellow signals. Representative images of both growth phases are displayed. Bar, 10  $\mu$ m.

the induction of hyphal-phase-specific genes is required to trigger hyphal formation or, rather, if hyphal induction is such a fast process that may be initiated, for example, by posttranslational modifications. Accordingly, a recent report demonstrated that phosphorylation of WASP in the acidic domain resulted in an increased affinity for the Arp2/3 complex, which was thus proposed to be required for WASP function (9). Understanding the signaling pathways in *C. albicans* that relay environmental signals to the actin cytoskeleton and result in the activation of key target proteins involved in the process of hyphal induction is thus one of the key fields of future research.

#### ACKNOWLEDGMENTS

We thank Joachim Ernst for providing plasmid libraries, Rong Li and Barbara Winsor for providing yeast strains, Ursula Oberholzer for discussions, Peter Philippsen for providing the heat stage, Manfred Barth (Zeiss, Jena) for his assistance in setting up the microscope, and Diana Schade for her excellent technical assistance.

J.W. is supported by the Deutsche Forschungsgemeinschaft, the Hans-Knöll Institut, and the Friedrich-Schiller University, Jena. Sequence data for *C. albicans* were obtained from the Stanford Genome Technology Center website at <http://www-sequence.stanford.edu/group/candida>. Sequencing of *C. albicans* was accomplished with the support of the NIDR and the Burroughs Wellcome Fund.

#### REFERENCES

1. Adamo, J. E., G. Rossi, and P. Brennwald. 1999. The Rho GTPase Rho3 has a direct role in exocytosis that is distinct from its role in actin polarity. *Mol. Biol. Cell* **10**:4121–4133.
2. Amberg, D. C., J. E. Zahner, J. W. Mulholland, J. R. Pringle, and D. Botstein. 1997. Aip3p/Bud6p, a yeast actin-interacting protein that is involved in morphogenesis and the selection of bipolar budding sites. *Mol. Biol. Cell* **8**:729–753.
3. Asleson, C. M., E. S. Bensen, C. A. Gale, A. S. Melms, C. Kurischko, and J. Berman. 2001. *Candida albicans* INT1-induced filamentation in *Saccharomyces cerevisiae* depends on Sla2p. *Mol. Cell. Biol.* **21**:1272–1284.
4. Bassilana, M., J. Blyth, and R. A. Arkowitz. 2003. Cdc24, the GDP-GTP exchange factor for Cdc42, is required for invasive hyphal growth of *Candida albicans*. *Eukaryot. Cell* **2**:9–18.
5. Bretscher, A. 2003. Polarized growth and organelle segregation in yeast: the tracks, motors, and receptors. *J. Cell Biol.* **160**:811–816.
6. Brown, A. J., and N. A. Gow. 1999. Regulatory networks controlling *Candida albicans* morphogenesis. *Trends Microbiol.* **7**:333–338.
7. Chang, F. S., C. J. Stefan, and K. J. Blumer. 2003. A WASP homolog powers actin polymerization-dependent motility of endosomes in vivo. *Curr. Biol.* **13**:455–463.
8. Cormack, B. P., R. H. Valdivia, and S. Falkow. 1996. FACS-optimized mutants of the green fluorescent protein GFP. *Gene* **173**:33–38.
9. Cory, G. O., R. Cramer, L. Blanchoin, and A. Ridley. 2003. Phosphorylation of the WASP-VCA domain increases its affinity for the Arp2/3 complex and enhances actin polymerization by WASP. *Mol. Cell* **11**:1229–1239.
10. EauClaire, S., and W. Guo. 2003. Conservation and specialization. The role of the exocyst in neuronal exocytosis. *Neuron* **37**:369–370.
11. Eitzen, G., L. Wang, N. Thorngren, and W. Wickner. 2002. Remodeling of organelle-bound actin is required for yeast vacuole fusion. *J. Cell Biol.* **158**:669–679.
12. Etienne-Manneville, S., and A. Hall. 2002. Rho GTPases in cell biology. *Nature* **420**:629–635.
13. Evangelista, M., B. M. Klebl, A. H. Tong, B. A. Webb, T. Leeuw, E. Leberer, M. Whiteway, D. Y. Thomas, and C. Boone. 2000. A role for myosin-I in actin assembly through interactions with Vrp1p, Bee1p, and the Arp2/3 complex. *J. Cell Biol.* **148**:353–362.
14. Evangelista, M., D. Pruyne, D. C. Amberg, C. Boone, and A. Bretscher. 2002. Formins direct Arp2/3-independent actin filament assembly to polarize cell growth in yeast. *Nat. Cell Biol.* **4**:260–269.
15. Evangelista, M., S. Zigmund, and C. Boone. 2003. Formins: signaling effectors for assembly and polarization of actin filaments. *J. Cell Sci.* **116**:2603–2611.
- 15a. Fonzi, W. A., and M. Y. Irwin. 1993. Isogenic strain construction and gene mapping in *Candida albicans*. *Genetics* **134**:717–728.
16. Gola, S., R. Martin, A. Walther, A. Dünkler, and J. Wendland. 2003. New modules for PCR-based gene targeting in *Candida albicans*: rapid and effi-

- cient gene targeting using 100bp of flanking homology region. *Yeast* **20**:1339–1347.
17. **Hazan, I., and H. Liu.** 2002. Hyphal tip-associated localization of Cdc42 is F-actin dependent in *Candida albicans*. *Eukaryot. Cell* **1**:856–864.
  18. **Hazan, I., M. Sepulveda-Becerra, and H. Liu.** 2002. Hyphal elongation is regulated independently of cell cycle in *Candida albicans*. *Mol. Biol. Cell* **13**:134–145.
  19. **Heath, I. B., G. Gupta, and S. Bai.** 2000. Plasma membrane-adjacent actin filaments, but not microtubules, are essential for both polarization and hyphal tip morphogenesis in *Saprolegnia ferax* and *Neurospora crassa*. *Fungal Genet. Biol.* **30**:45–62.
  20. **Hoepfner, D., A. Brachat, and P. Philippson.** 2000. Time-lapse video microscopy analysis reveals astral microtubule detachment in the yeast spindle pole mutant *cnm67*. *Mol. Biol. Cell* **11**:1197–1211.
  21. **Kost, B., E. Lemichez, P. Spielhofer, Y. Hong, K. Tolias, C. Carpenter, and N. H. Chua.** 1999. Rac homologues and compartmentalized phosphatidylinositol 4,5-bisphosphate act in a common pathway to regulate polar pollen tube growth. *J. Cell Biol.* **145**:317–330.
  22. **Leberer, E., D. Harcus, D. Dignard, L. Johnson, S. Ushinsky, D. Y. Thomas, and K. Schroppel.** 2001. Ras links cellular morphogenesis to virulence by regulation of the MAP kinase and cAMP signalling pathways in the pathogenic fungus *Candida albicans*. *Mol. Microbiol.* **42**:673–687.
  23. **Lechler, T., A. Shevchenko, and R. Li.** 2000. Direct involvement of yeast type I myosins in Cdc42-dependent actin polymerization. *J. Cell Biol.* **148**:363–373.
  24. **Lee, W. L., M. Bezanilla, and T. D. Pollard.** 2000. Fission yeast myosin-I, Myo1p, stimulates actin assembly by Arp2/3 complex and shares functions with WASp. *J. Cell Biol.* **151**:789–800.
  25. **Li, R.** 1997. Bee1, a yeast protein with homology to Wiscott-Aldrich syndrome protein, is critical for the assembly of cortical actin cytoskeleton. *J. Cell Biol.* **136**:649–658.
  26. **Liu, H., J. Kohler, and G. R. Fink.** 1994. Suppression of hyphal formation in *Candida albicans* by mutation of a *STE12* homolog. *Science* **266**:1723–1726.
  27. **Lo, H. J., J. Kohler, B. DiDomenico, D. Loebenberg, A. Cacciapuoti, and G. R. Fink.** 1997. Nonfilamentous *C. albicans* mutants are avirulent. *Cell* **90**:939–949.
  28. **Madania, A., P. Dumoulin, S. Grava, H. Kitamoto, C. Scharer-Brodbeck, A. Soulard, V. Moreau, and B. Winsor.** 1999. The *Saccharomyces cerevisiae* homologue of human Wiskott-Aldrich syndrome protein Las17p interacts with the Arp2/3 complex. *Mol. Biol. Cell* **10**:3521–3538.
  29. **Machesky, L.** 2000. The tails of two myosins. *J. Cell Biol.* **148**:219–221.
  30. **Machesky, L., and K. L. Gould.** 1999. The Arp2/3 complex: a multifunctional actin organizer. *Curr. Opin. Cell Biol.* **11**:117–121.
  31. **Marcil, A., D. Harcus, D. Y. Thomas, and M. Whiteway.** 2002. *Candida albicans* killing by RAW 264.7 mouse macrophage cells: effects of *Candida* genotype, infection ratios, and gamma interferon treatment. *Infect. Immun.* **70**:6319–6329.
  32. **Mayorga, M. E., and S. E. Gold.** 1999. A MAP kinase encoded by the *ubc3* gene of *Ustilago maydis* is required for filamentous growth and full virulence. *Mol. Microbiol.* **34**:485–497.
  33. **Morschhäuser, J., S. Michael, and J. Hacker.** 1998. Expression of a chromosomally integrated, single-copy GFP gene in *Candida albicans*, and its use as a reporter of gene regulation. *Mol. Gen. Genet.* **257**:412–420.
  34. **Müller, O., D. I. Johnson, and A. Mayer.** 2001. Cdc42p functions at the docking stage of yeast vacuole membrane fusion. *EMBO J.* **20**:5657–5665.
  35. **Naqvi, S. N., R. Zahn, D. A. Mitchell, B. J. Stevenson, and A. L. Munn.** 1998. The WASp homologue Las17p functions with the WIP homologue End5p/verprolin and is essential for endocytosis in yeast. *Curr. Biol.* **8**:959–962.
  36. **Oberholzer, U., A. Marcil, E. Leberer, D. Y. Thomas, and M. Whiteway.** 2002. Myosin I is required for hypha formation in *Candida albicans*. *Eukaryot. Cell* **1**:213–228.
  37. **Pruyne, D., and A. Bretscher.** 2000. Polarization of cell growth in yeast. *J. Cell Sci.* **113**:571–585.
  38. **Pruyne, D., M. Evangelista, C. Yang, E. Bi, S. Zigmund, A. Bretscher, and C. Boone.** 2002. Role of formins in actin assembly: nucleation and barbed-end association. *Science* **297**:612–615.
  39. **Roumanie, O., M. F. Peypouquet, D. Thoraval, F. Doignon, and M. Crouzet.** 2002. Functional interactions between the *VRP1-LAS17* and *RHO3-RHO4* genes involved in actin cytoskeleton organization in *Saccharomyces cerevisiae*. *Curr. Genet.* **40**:317–325.
  40. **Sagot, I., A. A. Rodal, J. Moseley, B. L. Goode, and D. Pellman.** 2002. An actin nucleation mechanism mediated by Bni1 and profilin. *Nat. Cell Biol.* **4**:626–631.
  41. **Seeley, E. S., M. Kato, N. Margolis, W. Wickner, and G. Eitzen.** 2002. Genomic analysis of homotypic vacuole fusion. *Mol. Biol. Cell* **13**:782–794.
  42. **Ushinsky, S. C., D. Harcus, J. Ash, D. Dignard, A. Marcil, J. Morschhäuser, D. Y. Thomas, M. Whiteway, and E. Leberer.** 2002. *CDC42* is required for polarized growth in human pathogen *Candida albicans*. *Eukaryot. Cell* **1**:95–104.
  43. **Vida, T. A., and S. D. Emr.** 1995. A new vital stain for visualizing vacuolar membrane dynamics and endocytosis in yeast. *J. Cell Biol.* **128**:779–792.
  44. **Walther, A., and J. Wendland.** 2003. An improved transformation protocol for the human fungal pathogen *Candida albicans*. *Curr. Genet.* **42**:339–343.
  45. **Wendland, J.** 2001. Comparison of morphogenetic networks of filamentous fungi and yeast. *Fungal Genet. Biol.* **34**:63–82.
  46. **Wendland, J.** 2003. PCR-based methods facilitate gene manipulations and cloning procedures. *Curr. Genet.* **44**:115–123.
  47. **Wendland, J., and P. Philippson.** 2000. Determination of cell polarity in germinated spores and hyphal tips of the filamentous ascomycete *Ashbya gossypii* requires a rhoGAP homolog. *J. Cell Sci.* **113**:1611–1621.
  48. **Wendland, J., and P. Philippson.** 2001. Cell polarity and hyphal morphogenesis are controlled by multiple rho-protein modules in the filamentous ascomycete *Ashbya gossypii*. *Genetics* **157**:601–610.
  - 48a. **Wilson, R. B., D. Davis, and A. P. Mitchell.** 1999. Rapid hypothesis testing with *Candida albicans* through gene disruption with short homology regions. *J. Bacteriol.* **181**:1868–1874.
  49. **Winter, D., A. V. Podtelejnikov, M. Mann, and R. Li.** 1997. The complex containing actin-related proteins Arp2 and Arp3 is required for the motility and integrity of yeast actin patches. *Curr. Biol.* **7**:519–529.
  50. **Winter, D. C., E. Y. Choe, and R. Li.** 1999. Genetic dissection of the budding yeast Arp2/3 complex: a comparison of the in vivo and structural roles of individual subunits. *Proc. Natl. Acad. Sci. USA* **96**:7288–7293.
  51. **Yang, S., K. R. Ayscough, and D. G. Drubin.** 1997. A role for the actin cytoskeleton of *Saccharomyces cerevisiae* in bipolar bud-site selection. *J. Cell Biol.* **136**:111–123.
  52. **Yokoyama, K., H. Kaji, K. Nishimura, and M. Miyaji.** 1990. The role of microfilaments and microtubules in apical growth and dimorphism of *Candida albicans*. *J. Gen. Microbiol.* **136**:1067–1075.